Parquin and Carboxyparquin, Toxic Kaurene Glycosides from the Shrub *Cestrum parqui*

Clive M. Pearce,[a] Nicholas J. Skelton,[a] Stephen Naylor,[b] Rajamoorthi Kanaan,[a] Janice Kelland,[a] Peter B. Oelrichs,[c] Jeremy K. M. Sanders *[,a] and Dudley H. Williams *[,a]

[a] *Cambridge Centre for Molecular Recognition, University Chemical Laboratory, Lensfield Road, Cambridge CB2 1EW, UK*

[b] *MRC Toxicology Unit, Medical Research Council Laboratory, Woodmansterne Road, Carshalton, Surrey SM5 4EF, UK*

[c] *Animal Research Institute, 665 Fairfield Road, Yeerongpilly, Queensland 4105, Australia*

Two kaurene glycosides have been isolated from the dried leaves of the shrub *Cestrum parqui*, a common weed in parts of South America and Australia, and their structures determined by modern NMR and mass spectrometry techniques. These compounds, named carboxyparquin and parquin, differ only by one carboxylic acid group at C-4. The former is believed to be responsible for widespread poisoning of grazing animals in these areas; the latter appears to be a relatively non-toxic co-metabolite. There is a close structural similarity between these compounds and carboxyatractyloside and atractyloside, which are known toxins with strychnine-like action, isolated from *Atractylis gummifera L.* The parquins possess a different pyranose ring from the atractylosides and an additional γ-lactone, both with unprecedented functionality.

Cestrum parqui L'Herit.1788 (Solanaceae), a perennial shrub native to South America, is now naturalised and a common weed in eastern mainland Australia.[1] Sporadic cases of cattle poisoning by the plant have been reported from both South America[2–4] and Australia.[5,6] Poisoning of sheep, horses, pigs and poultry is also documented.[7] The principal lesion in poisoned cattle is severe periacinar coagulation necrosis of hepatocytes in the liver.[3,6] A similar pattern of liver necrosis is seen in poisoning by several plant species including some of those in the genera *Trema*, *Xanthium*, *Myoporum* and *Hertia*,[7,8] in poisoning by cyanobacteria (blue–green alga)[9] and by larvae of sawflies.[10,11]

By a series of extractions and chromatography steps, an active component has been isolated from the dried leaves of the shrub. In mice, this purified toxin is over 50 times more toxic than the crude extracts of the leaf. The approximate LD50 for carboxyparquin in mice was found to be 4.3 mg Kg^{-1}, and this produced both kidney and liver lesion of the sort seen after intoxication of this species with the crude *C. parqui* extract.[12] We now report the structure of the toxic component **1** which we have called carboxyparquin. We have also isolated and identified the co-metabolite **2** which has a remarkably similar structure but which is relatively non-toxic; no abnormality was observed in mice given this compound at four times the dose rate of **1**, although toxicity may be observed at higher dose rates. We have called this second component parquin.

Mass spectrometry (MS) and nuclear magnetic resonance (NMR) techniques have been the main tools used in determining these structures. The fast atom bombardment (FAB) MS technique allowed observation of both molecular ions and diagnostic fragment ions for these high molecular weight (798 and 754 Da) and polar materials. Investigations were carried out in both the positive and negative ion modes. Homonuclear two-dimensional (2D) ^1H NMR spectroscopy was used to identify isolated coupling networks and these were linked together using a combination of ^1H nuclear Overhauser effects (NOEs) and long-range (2–3 bond) ^{13}C–^1H correlation experiments. The NOE observations also allow most of the stereochemical relationships to be established as well as indicating conformational preferences.

The enormous information content of modern spectroscopic techniques has meant that it has been possible to work with **1** and **2** as intact molecules and so reduce chemical degradation and derivatization to a minimum. For reasons of clarity, and to reflect the chronological order of the work, details of structure elucidation in this report are confined mainly to **1**. Indeed, the co-metabolite **2** only became available once a tentative structure had been proposed for **1**. Preliminary spectroscopic investigation of **2** soon made its structural similarity to **1** apparent, and more detailed analysis provided complementary data such that the structures of both molecules could be deduced.

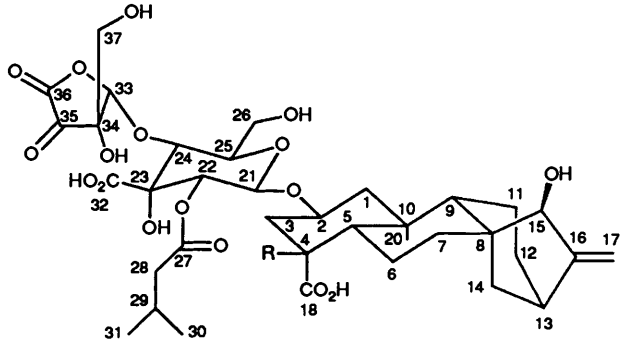

1 R = CO_2H (C-19) : carboxyparquin
2 R = H : parquin

Results

The structure determination of **1** is described in three stages: first, a survey of evidence gathered from preliminary MS, NMR, infrared (IR), ultraviolet (UV) and microanalysis experiments; second, a detailed study of the NMR investigations which constitute the basis of the determination and lead to the proposed structure; and third, a confirmatory look at all data including those obtained from the co-metabolite **2**.

Preliminary Survey.—FAB-MS in the positive ion mode, using a variety of different matrices, consistently shows the highest mass ions of significant abundance (other than matrix

Table 1 ^{13}C NMR data for **1** and **2** in D_2O at 298 K

Compound 1			Compound 2	
Carbon	Chemical Shift (ppm) (multiplicity, J/Hz)[a]	Long-range (2–3 bond) ^{13}C–^{1}H correlations[b]	Carbon	Chemical shift (ppm)
35	201.5 (s)	37a	35	201.2
19	179.3 (s)	—	18	180.8
18	178.8 (s)	3b, 5	27	175.1
27	175.0 (s)	22, 28a, 28b, 29	36	172.5
36	172.6 (s)	33	32	171.6
32	171.0 (s)	—	16	159.5
16	159.7 (s)	14a, 17a, 17b	17	109.2
17	109.3 (t, 154)	15	21	98.1
21	98.8 (d, 166)	22	33	93.2
33	93.4 (d, 166)	—	34	89.6
34	89.8 (s)	33, 37a	15	83.0
15	83.0 (d, 157)	14a, 17a, 17b	2	74.8
2	75.2 (d, 146)	1a, 1b, 3a, 3b, 21	24	74.4
24	74.2 (d, 146)	33	25	72.2
25	72.4 (d, 146)	26a, 26b	22	70.4
22	69.9 (d, 147)	21, α	23	69.6
23	69.8 (s)	α	26	60.7
4	61.3 (s)	3a, 3b, 5	37	57.8
26	60.8 (t, 146)	—	9	52.9
37	58.0 (t, 143)	—	5	49.2
9	53.6 (d, 123)	1b, 14b, 15, 20, γ,	8	47.9
5	52.2 (d, 127)	1a, 1b, 20, β	1	47.3
8	48.2 (s)	6a, 9, 13, 14a, 14b, β, γ	4	44.2
1	47.2 (t, 127)	3a, 9, 20	28	43.0
28	43.2 (t, 130)	29, δ	13	42.6
13	42.8 (d, 137)	14b, 15, 17a, 17b	10	40.9
10	40.7 (s)	5, 9, 20, β, γ	14	36.4
3	40.5 (t, 131)	1a	11	35.2
14	36.6 (t, 131)	9, 15	3	34.6
11	35.6 (t, 121)	9, γ	12	32.7
12	32.0 (t, 127)	9, 14b, γ	6	25.6
29	25.6 (d, 130)	28a, 28b, δ	29	25.4
6	23.6 (t, 110)	—	30/31	22.7
30/31	22.8 (q, 125)	28a, 28b, 29	30/31	22.5
30/31	22.6 (q, 125)	28a, 28b, 29	7	18.5
7	18.7 (t, 120)	5, 9, 14b	20	16.6
20	17.6 (q, 125)	1, 5, 9		

[a] Convention used: s, singlet; d, doublet; t, triplet; q, quartet. [b] For convenience, α, β, γ, δ represent groups of coincident proton resonances (as shown in Table 2) where: α = 24-H, 25-H; β = 6b-H, 7a-H, 11a-H, 12a-H; γ = 7b-H, 11b-H, 12b-H; δ = 30-H, 31-H.

oligomer ions) to be at m/z 837, 821, 816 and 799 although these are of low relative abundance, particularly the last. However, in the negative ion mode using glycerol or 3-nitrobenzyl alcohol as the matrix, the highest mass ion of significant abundance is seen at m/z 797 as an intense peak. In some sample preparations, a less abundant peak was also observed at m/z 819, the mass difference between these two ions implying the formation of a sodium adduct. Such adducts are rare in negative ion FAB-MS and this suggests that **1** has a high affinity for cations. The high mass ions seen in the positive ion mode would thus be consistent for the potassium, sodium, ammonium and protonated adducts of a material with a molecular weight of 798 Da; the very low abundance of the ion at m/z 799 ($[M + H]^+$) bears out the affinity of the molecule for cations. In the negative ion mode, fragment ions are much more abundant; however, at this stage no inferences are drawn from these ions.

When **1** is lyophilized from D_2O (three times), the negative mode pseudo-molecular ion appears at m/z 804. This increase of seven mass units is indicative of eight exchangeable hydrogens, assuming that one of the labile hydrogen sites holds the formal negative charge of the pseudo-molecular ion. Microanalysis of **1** did not give an unambiguous molecular formula, but demonstrated that carbon, hydrogen and oxygen are the only elements present; therefore the eight exchangeable hydrogens must be present as hydroxy or carboxylic acid groups. Small scale acylation (pyridine–acetic anhydride) raises the positive mode pseudo-molecular ion by 210 mass units, indicating five hydroxy functions. By difference this implies three carboxylic acid groups; this is confirmed by esterification (diazomethane or methyl iodide–potassium carbonate) and subsequent FAB-MS.

Notable features of the ^{1}H and ^{13}C NMR spectra are the absence of aromatic resonances and the two well separated groups of ^{1}H signals. This latter observation, when taking the ^{1}H chemical shifts into account, suggests the presence of polar and non-polar moieties within the molecule. The chemical shifts of all 37 carbon atoms are presented in Table 1, with assignments corresponding to the carbon numbering shown for **1**. DEPT and one-bond ^{13}C–^{1}H correlation NMR experiments establish carbon type and correlate all the 42 ^{1}H resonances observed in D_2O. This information is also included in Table 1 along with $^{1}J_{CH}$ values obtained from a ^{1}H-detected ^{1}H–^{13}C correlation experiment, which was acquired ^{1}H-coupled. Table 2 shows the chemical shifts, multiplicity and coupling constants of these carbon-bound hydrogens. Several signals in the high field group of resonances are not sufficiently well dispersed to allow accurate measurement of their coupling constants from the one-dimensional (1D) spectrum. Where this is the case, approximate values obtained from DQF-COSY experiments can be found in parenthesis in Table 3 (referred to later).

Based on the above knowledge we can propose a molecular formula of $C_{37}H_{50}O_{19}$ for **1**. In the ^{13}C NMR spectrum, it is possible to identify six carbonyl carbons (δ 210–160, including

Table 2 1H NMR data for **1** and **2** in D_2O at 298 K

Compound **1**		Compound **2**	
Proton	Chemical shift (ppm) (multiplicity, *J*/Hz)[a]	Proton	Chemical shift (ppm) (multiplicity, *J*/Hz)[a]
33	5.30 (s)	33	5.36 (s)
17a	5.15 (d, 3.0)	17a	5.24 (d, 3.0)
17b	5.11 (d, 3.0)	17b	5.11 (d, 3.0)
21	4.96 (d, 7.6)	21	5.06 (d, 7.9)
22	4.65 (d, 7.6)	22	4.72 (d, 7.9)
37a	4.41 (d, 13.1)	37a	4.47 (d, 12.9)
2	4.17 (o)	2	4.30 (m)
37b	4.05 (d, 13.1)	37b	4.15 (d, 12.9)
24/25[b]	4.00 (bs)	24/25[b]	4.07 (bs)
15	3.88 (bs)	15	3.92 (bs)
26a	3.86 (d, 13.2)	26a	3.86 (d, 12.4)
26b	3.72 (dd, 13.2, 3.0)	26b	3.78 (dd, 12.4, 3.0)
13	2.72 (bs)	13	2.79 (bs)
3a	2.49 (dd, 13.1, 2.6)	4	2.77 (o)
28a	2.33 (dd, 13.1, 2.6)	1a/3a/28a/28b[b]	2.35 (m)
1a	2.29 (o)	29	2.10 (sep, 6.9)
28b	2.24 (o)	14a	1.94 (d, 12.4)
29	2.00 (sep, 6.9)	6a	1.86 (q, 12.5)
14a	1.88 (d, 12.1)	6b/7a/11a/12a[b]	1.66 (m)
6a	1.84 (q, 12.4)	5/7b/11b/12b[b]	1.50 (m)
5	1.67 (bd, 12.4)	14b	1.38 (dm, 12.4)
6b/7a/11a/12a[b]	1.59 (m)	3b	1.23 (td, 12.9, 5.9)
7b/11b/12b[b]	1.54 (m)	9	1.11 (bd, 6.5)
14b	1.28 (dm, 12.1)	30(31)[c]	1.04 (d, 6.9)
3b	1.26 (td, 13.1, 6.0)	31(30)[c]	1.01 (d, 6.9)
9	1.14 (bd, 6.1)	20	1.00 (s)
30/31[b]	0.98 (bd, 6.9)	1b	0.79 (t, 12.5)
20	0.95 (s)		
1b	0.79 (t, 12.4)		

[a] Convention used: s, singlet; d, doublet; t, triplet; q, quartet; sep, septet; o, obscured; b, broad; m, multiplet. Only the larger and most easily measurable couplings are presented. Many more couplings are seen in the DQF-COSY experiments. [b] Coincident resonances. [c] Methyl groups show conformational preference but cannot be distinguished from each other.

one ketone-like carbon at δ 201), 17 aliphatic carbon atoms (δ 45–10) and 14 other carbon atoms (δ 160–60, probably attached to oxygens). As seen in Table 1, the DEPT experiments show three methyl groups, eleven methylene carbons, eleven methine carbons and twelve quaternary carbons. UV and IR spectroscopies allow no significant gain in headway from this point; there is no UV chromophore with an absorption above 240 nm and the IR peaks are broad and generally uninformative. Hydroxy groups are suggested by a strong broad peak at 3420 cm^{-1}, and carboxylic acid groups by a very broad peak at around 3000 cm^{-1} with sharper peaks at 1626 and 1400 cm^{-1}. A relatively sharp peak seen at 1723 cm^{-1} is suggestive of the carbonyl stretch of a ketone or ester.

Attempts to view all five proposed hydroxy protons by acquiring ^1H spectra in dry DMSO did not prove entirely satisfactory; only three such protons could be detected, presumably due to fast exchange of the others with residual water. The spectra suffer from increased line-broadening in this solvent.

NMR Study.—All the ^1H–^1H scalar coupling connectivities seen in both magnitude mode COSY and phase-sensitive DQF-COSY experiments are presented in Table 3. The weakest correlations were not observed in DQF spectra where the signal–noise ratio is worse by a factor of $\sqrt{2}$.[13] From the latter, coupling constants have been estimated[14] and this information has been used in conjunction with the coupling constants shown in Table 2. Relatively few NOEs (all positive) were observed in NOE-difference and NOESY experiments, almost certainly due to the adverse correlation time of the molecule. The problem was removed by the use of 2D CAMELSPIN[15,16] experiments and the NOEs from these experiments are also shown in Table 3.

The pair of signals at δ 5.15 and 5.11 present a good starting point for the investigation of the proton spin systems. These signals form a geminal pair, attached to a carbon with a ^{13}C resonance at δ 109.3 (C-17). The 3 Hz geminal coupling constant plus the ^1H and ^{13}C chemical shifts strongly suggest olefinic character. Both of these resonances (17a-H and 17b-H) show small couplings to ^1H signals at δ 3.88 (15-H) and 2.72 (13-H). Proton 17b-H also shows a very small coupling to a ^1H signal at δ 1.88 (14a-H) which has a geminal partner at δ 1.28 (14b-H). A small coupling between 14a-H and 15-H and a larger coupling linking 13-H to 14b-H leads to the part structure **A** when consideration is made of chemical shift and coupling constants.

Continuing in this manner, using both scalar and dipolar coupling connectivities allows **A** to be extended to part structure **B**. A HOHAHA[17] experiment was required to overcome the problem of resonance overlap encountered with the C-11 and C-12 methylenes. Also, long-range ^{13}C–^1H correlation experiments, which utilise the heteronuclear coupling operating over at least two bonds, were employed to establish quarternary carbons C-4, C-8, C-10 and C-16 within this structure. All such long-range ^{13}C–^1H coupling correlations are included in Table 1 and these further serve to support part structure **B**. The skeleton of fragment **B** is based upon that of kaurene **3** which occurs naturally in both enantiomeric forms, (+)-kaurene and (−)-*ent*-kaurene.[18] Relative to kaurene, modifications have clearly occurred at C-2 and C-15 where oxygen atoms are now attached, and at C-4 where the methyl groups have been replaced. The chemical shift of C-4 (δ 61.3) and the fact that the most prominent fragment ion in the negative ion FAB-MS spectrum of **1** is at *m/z* 363, is consistent with the attachment of two carboxylic acid groups on C-4.

Table 3 The scalar and dipolar coupling connectivities of **1** seen in COSY and NOE experiments

Protons	Protons connected[a] by scalar coupling	Protons connected[b] by dipolar coupling
33	37a (s), 37b (s)	α (1), 37a (m), 37b (s)
17a	13 (s), 14a (s), 15 (s), 17b (m)	15 (s), 17b (1)
17b	13 (s), 15 (s), 17a (m)	13 (m), 17a (1)
21	22 (1)	2 (m), α (1), 37a (s)
22	21 (1)	α (1), 37a (m), 37β (1)
37a	33 (s), 37b (1)	22 (m), α (m), 37b (1)
2	1a (m), 1b (1), 3a (m), 3b (1)	1a (s), 3a (s), 21 (m)
37b	33 (s), 37a (1)	22 (1), 33 (s), 37a (1)
24/25[c]	26a (s), 26b (s)	21 (m), 22 (m), 33 (s), 37a (s), 37b (m)
15	14a (s), 17a (s), 17b (s)	9 (1), β (s), γ (s)
26a	α (s), 26b (1)	
26b	α (m), 26a (1)	
13	14b (m), 17a (s), 17b (s), β (s), γ (s)	14a (s), 17b (m), β (m), γ (m)
3a	1a (s), 2 (m), 3b (1)	2 (s), 3b (1), 21 (s)
28a	28b (1), 29 (m), δ (s)	
1a	1b (1), 2 (m), 3a (s)	1b (1), 9 (s), β (s)
28b	28a (1), 29 (m), δ (s)	
29	28a (m), 28b (m), δ (m)	
14a	14b (1), 15 (s), 17a (s)	13 (s), 14b (1), 20 (m)
6a	5 (m), β (1), γ(m)	
5	6a (m), 20 (s), β (m), γ (s)	1b (s), 3b (s), 9 (s)
6b/7a/11a/12a[c]	5 (m), 6a (1), 13 (s), γ (1)	
7b/11b/12b[c]	6a (1), 9 (s), 13 (s), β (1)	
14b	13 (m), 14a (1)	14a (1)
3b	2 (1), 3a (1)	5 (s)
9	20 (s), γ (m)	1b (m), 5 (s), 15 (1), β (s), γ (s)
30/31[c]	28a (s), 28b (s), 29 (m)	
20	1b (s), 5 (s), 9 (s)	2 (s), 14a (s), β (s), γ (s)
1b	1a (1), 2 (1), 20 (s)	1a (1), 5 (s), 9 (m)

[a] Size of coupling estimated from DQF–COSY experiments where: s, small (0–3 Hz); m, medium (3–7 Hz); l, large (>7 Hz). [b] Size of NOE subjectively listed as: s, small (1–5%); m, medium (5–10%); l, large (>10%). [c] For convenience, coincident proton resonances appear in the table according to: α = 24-H, 25-H; β = 6b-H, 7a-H, 11a-H, 12a-H; γ = 7b-H, 11b-H, 12b-H; δ = 30-H, 31-H.

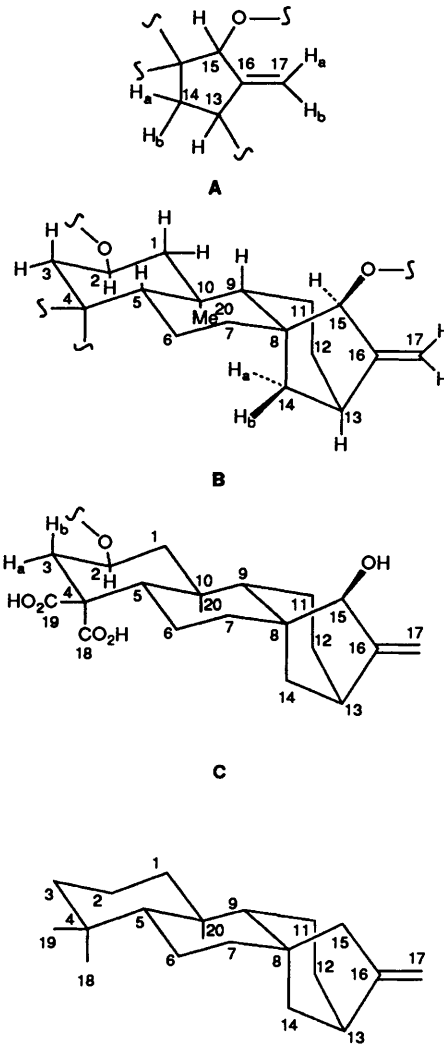

3 kaurene [(−)-*ent*-kaurene depicted]

These conclusions lead to the part structure **C** and are supported by long-range ^{13}C–^{1}H correlations.

Fragment **C** gives NOEs from only two of its protons (2-H and 3a-H) to a proton (21-H) in another part of the molecule. On the basis of the chemical shift, C-21 is though to be anomeric so a glycosidic bond links C-2 and C-21. There is a reasonably large coupling (7.6 Hz) but no NOE between 21-H and 22-H, which indicates an antiperiplanar arrangement of these protons, consistent with them belonging to a six membered ring. Piecing the remainder of the molecule together was primarily achieved by extensive use of several ^{13}C–^{1}H correlation spectra where delays in the pulse sequence were adjusted to optimise couplings throughout the range 2–15 Hz. Such spectra demonstrate the presence of a coupling but do not allow its measurement.

These data show a small coupling between C-2 and 21-H (not however between C-21 and 2-H). Additionally, the carbonyl carbon C-27 is coupled to 22-H, 28a-H, 28b-H and 29-H, showing it belongs to an isovalerate fragment linked to C-22. Clearly, carbons C-23, C-24, C-25 and C-26 are also contained in this portion of the molecule. Consideration of these observations and re-examination of the ^{1}H NOEs operating between 21-H, 22-H, 24-H, 25-H, 26a-H and 26b-H lead to the modified pyranose ring shown in part structure **D**.

A very small coupling between C-24 and 33-H connects **D** to the final portion of the molecule, which is seen to include carbon centres C-33, C-34, C-35, C-36 and C-37. This accounts for all but one of the remaining carbons, which must therefore be one of the carbonyls seen at δ 179.3 and 171.0. We know that one of these belongs to the carboxylate group which displays no connectivity but which resides on C-4 of the kaurene fragment, *i.e.*, C-19. We also know that the molecule contains three carboxylic acid groups and therefore conclude that the third acid function resides on C-23 of the pyranose ring and thereby accounts for this other carbonyl and final carbon atom, *i.e*, C-32.

The final portion of the molecule comprises of an anomeric carbon (C-33), a quaternary carbon attached to an oxygen (C-34), two carbonyls (C-35 and C-36) and a methylene attached to an oxygen (C-37). Oxygen attachment is deduced from ^{1}H and ^{13}C chemical shifts.

Very small scalar ^{1}H couplings (indicative of $^{4}J_{HH}$) connect the anomeric 33-H to the methylene pair, 37a-H and 37b-H. NOEs also show these to be in close spatial proximity and, by virtue of strong mutual enhancements, indicate that a preferred conformation has 22-H and 24-H of the pyranose nearby.

In the long-range (2–3 bond) ^{13}C–^{1}H correlation experiments, C-24 of the pyranose moiety is seen to couple to 33-H, whereas no coupling is seen between C-33 and 24-H, 37a-H or 37b-H. The quaternary, C-34 couples to both 33-H and 37a-H. From its chemical shift (δ 201.5), C-35 is reasoned to be ketonic and is seen to couple to 37a-H. By contrast, C-36 (δ 172.6) is clearly of acid, ester or lactone type and has a coupling to 33-H. No

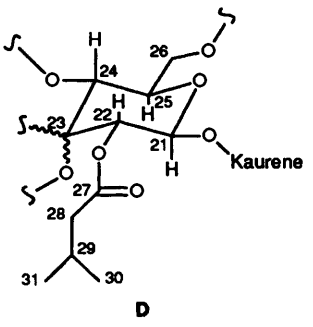

D

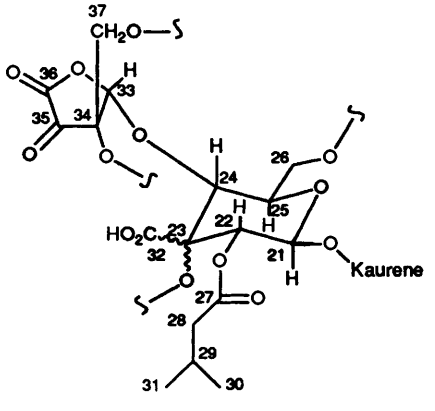

E

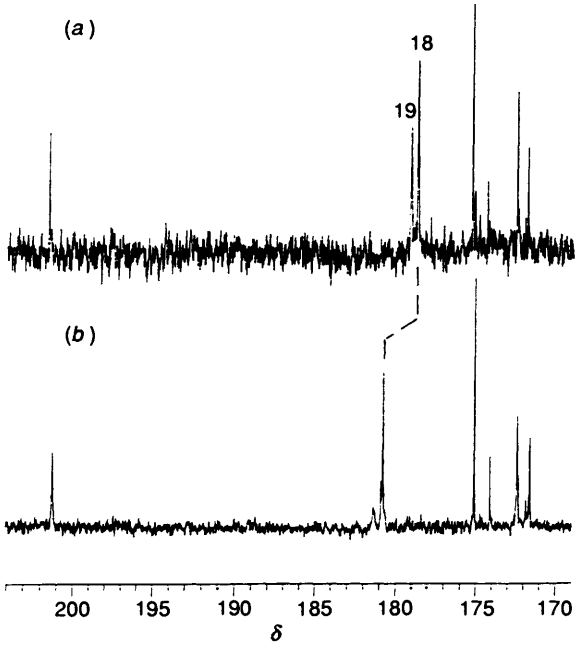

Fig. 1 Low-field, carbonyl, regions of the ^{13}C spectra of **1** and **2**: (*a*) compound **1** showing six carbonyls; (*b*) compound **2** showing the absence of C-19 and the change in chemical shift of C-18. The smaller peaks are due to impurities.

coupling could be found between the methylene C-37 (the final carbon in this portion of the molecule) and 33-H.

The above evidence is best accommodated by the γ-lactone shown in part structure **E**.

Already, one of the five hydroxy groups of the molecule has been assigned to C-15 of the kaurene system. The remaining four can now be assigned to C-23, C-26, C-34 and C-37 of the pyranose and lactone rings. We therefore propose the gross structure of carboxyparquin **1**.

At this stage we turned our attention to the non-toxic (or less

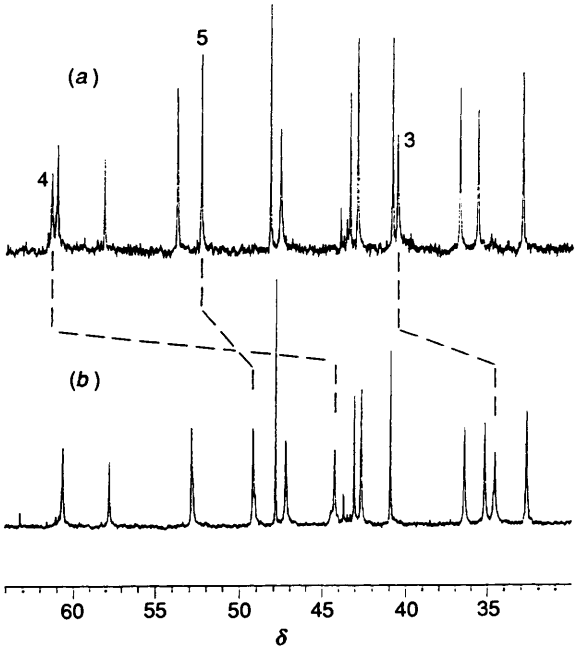

Fig. 2 High-field regions of the ^{13}C spectra of **1** and **2** where the major differences occur: (*a*) compound **1**; (*b*), compound **2**, showing the changes in chemical shifts of C-3, C-4 and C-5 (C-4 is a quaternary carbon in **1** and a methine carbon in **2**). As in Fig. 1, the smallest peaks are from impurities.

toxic) component **2**. Fortunately, this proved to be closely related to **1** and the work undertaken provides confirmatory evidence for the structure **1**, as described below.

Confirmation of the Structure of **1** *and Examination of the Co-metabolite* **2**.—The ^1H and ^{13}C NMR spectra of **2** are very similar to those of **1** with the most striking differences observed in the ^{13}C spectra (Figs. 1 and 2). One less carbon is revealed in the spectrum of **2** since the carbonyl C-19 of the carboxylic acid group assigned to the equatorial position on C-4 in **1** is absent. The chemical shifts of all 36 carbon atoms are presented in Table 1, with assignments corresponding to the carbon numbering shown for **2**. Compared with **1**, there is one extra methine carbon (δ 44.2), while the quaternary C-4 in **1** is now absent and significant chemical shift changes have occurred at C-3, C-5 and C-18. The new methine resonance correlates to the additional ^1H signal seen at δ 2.77. Table 2 includes the chemical shifts, multiplicity and coupling constants of the 43 carbon-bound protons in **2**. Clearly, the equatorial carboxylic acid group present at C-4 in **1** has been replaced by a single proton in **2**. Examination of the DQF-COSY spectrum of **2** shows 4-H has two relatively large couplings (*ca.* 7 Hz; ax–eq) to 5-H and 3b-H and one small coupling (*ca.* 2 Hz; eq–eq) to 3a-H. This is consistent with the stereochemistry and conformation expected for the kaurene system. The presence of this proton at C-4 allows the complete ^1H coupling network of the kaurene to be mapped out. Reassuringly, all the relative stereochemical and conformational aspects of the kaurene ring system of **1** are also found for **2**. The ^1H–^1H coupling seen in the modified pyranose and lactone portions is identical for both structures and no new information is obtained from long-range ^{13}C–^1H correlation experiments with **2**.

FAB-MS on **2** in the positive ion mode, using a glycerol matrix, reveals the highest mass ion of significant abundance to be at *m/z* 793. The molecular weight of **2** is 754 Da and so this ion corresponds to the potassium adduct $[(M + K)^+]$. Similarly, ions at *m/z* 777 and 772 are consistent with the sodium and ammonium adducts. Only one significant fragment ion is observed at *m/z* 435 and when the positive FAB-MS data

Table 4 Major ions seen in negative FAB-MS of **1** and **2** using glycerol as the matrix

Compound **1**		Compound **2**	
Ions observed[a]	Assignment	Ions observed[a]	Assignment
819 (m)	$[M - 2H + Na]^-$	791 (s)	$[M - 2H + K]^-$
797 (vl)	$[M - H]^-$	775 (m)	$[M - 2H + Na]^-$
779 (s)	$[M - H - H_2O]^-$	753 (vl)	$[M - H]^-$
753 (m)	$[M - H - CO_2]^-$	735 (m)	$[M - H - H_2O]^-$
694 (s)	$[M - H - C_4H_9CO_2]^-$	708 (s)	$[M - H - CO_2H]^-$
363 (l)	$[kaurene]^-$	663 (m)	$[M - H - 2CO_2H]^-$
319 (l)	$[kaurene - CO_2]^-$	319 (l)	$[kaurene]^-$
301 (m)	$[kaurene - CO_2 - H_2O]^-$	275 (l)	$[kaurene - CO_2]^-$
101 (l)	$[C_4H_9CO_2]^-$	257 (s)	$[kaurene - CO_2 - H_2O]^-$
		101 (l)	$[C_4H_9CO_2]^-$

[a] Intensity subjectively listed according to: vl, very large; l, large; m, medium; s, small.

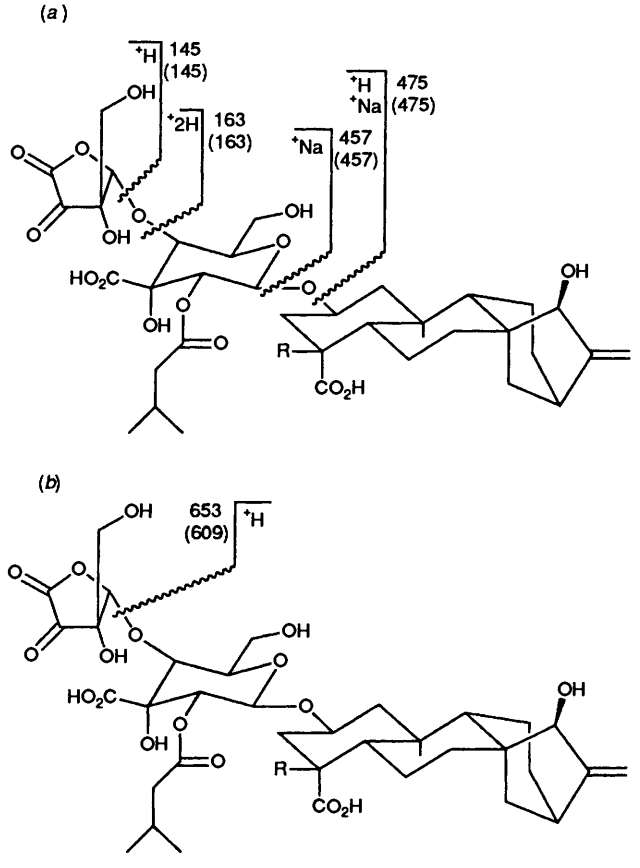

Fig. 3 Abundant daughter ions, formed by CAD, and observed in the tandem mass spectra of **1** and **2** (ions formed from **2** are shown in parenthesis): (*a*), positive ions from $[M + Na]^+$; (*b*), negative ions from $[M - H]^-$.

on **1** is re-examined this ion is again the only significant fragment ion detected. This ion must therefore correspond to loss of the kaurene moieties in both cases. The negative ion FAB-MS spectrum of **2** shows an abundant pseudo-molecular ion at *m/z* 753 ($[M - H]^-$) and the rest of the spectrum corresponds well with that obtained from **1**. More peaks are observed than in the positive ion mode and assignments for the most prominent of these appear in Table 4.

Tandem MS[19] studies on both **1** and **2** have proved particularly useful in that evidence for the three ring systems (kaurene, pyranose and lactone) is provided in both cases. Subjecting the positive ions seen at *m/z* 821 ($[M + Na]^+$) for **1** and at *m/z* 777 ($[M + Na]^+$) for **2** and the negative ions seen at *m/z* 797 ($[M - H]^-$) for **1** and at *m/z* 753 ($[M - H]^-$) for **2** to collision activated dissociation (CAD) resulted in the formation of the daughter ions (ions formed by direct fragmentation of these parent ions) depicted in Fig. 3. These prove to be very informative and are consistent with the fragmentation expected for **1** and **2** (Fig. 3 provides a self-explanatory account of this).

There remains a stereochemical uncertainty over the arrangement of the hydroxy and carboxylic acid functions at C-23. There is no 3-bond coupling from the carbonyl of the acid group to either 22-H or 24-H. Such a coupling would be expected if the carboxylic acid group were axial (compare with C-4, where the carbonyl of the axial acid couples to both axial proton neighbours (3b-H and 5-H), whereas no coupling is observed involving the carbonyl of the equatorial acid group). Thus we propose the relative stereochemistry shown, where the carboxylic acid group is equatorial and the hydroxy is axial.

There is a close similarity of **1** and **2** to carboxyatractyloside **4** and atractyloside **5**. These compounds are of known absolute

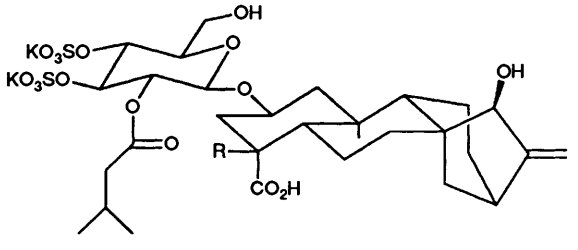

4 R = CO_2H : carboxyactractyloside
5 R = H : actractyloside

stereochemistry[20,21] and are highly toxic, producing strychnine-like symptons.[22] The kaurene part of these molecules has been shown to be of the same absolute stereochemistry as (−)-*ent*-kaurene and the hexose ring has been determined as being of D-configuration. Based on these analogies, the structures of **1** and **2** are drawn with these stereochemistries. However, the absolute stereochemistry of the γ-lactone remains undefined.

Experimental

Plant Material.—The plant material used in this study was collected in the winter of 1983 from an area in Southeastern Queensland where stock poisoning had recently occurred. A specimen submitted to the Botany Branch, Queensland Department of Primary Industries was identified as *Cestrum parqui* L'Herit (Herbarium Voucher Number BRI 308 531). Fresh green leaves separated from the stems were oven dried at 60 °C for 18 h, and then pulverised in a hammer mill. This material was stored at room temperature in plastic containers.

Isolation and Purification.—Dried milled leaf (200 g) was extracted (×3) with hot EtOH–H_2O (1:1) containing 1% NH_4OH. The combined extracts were concentrated to 200 cm^3, and extracted (×5) with BuOH. The combined BuOH extracts were washed (×2) with H_2O, and the BuOH was discarded. The combined aqueous solutions were evaporated under reduced pressure to remove the BuOH, acidified to pH 5–6 with H_2SO_4 and added to a polyamide column (100 g). The column was washed with H_2O until neutral, followed by EtOH–H_2O (1:1) (500 cm^3) and 1% NH_4OH (500 cm^3). The NH_4OH eluates were combined and dried under reduced pressure, the residue was dissolved in EtOH–H_2O (1:1) containing 1% NH_4OH (20 cm^3), and added to an LH-20 column (2 × 70 cm). Fractions (20 cm^3) were collected, and those containing the toxin evaporated to dryness under reduced pressure. The impure toxin was then added to an XAD-2 column (particle size 0.05–0.1 mm) (2 × 90 cm) in H_2O, and the column washed with H_2O (1 dm^3), followed by a gradient of MeOH in H_2O. Fractions (20 cm^3) were collected and compound **1** (carboxyparquin) and compound **2** (parquin) were shown to be completely resolved by TLC using Merck Kieselgel 60. Solvent systems (i), upper phase of BuOH–AcOH–H_2O (4:1:5); (ii), BuOH–MeOH–pyridine–H_2O (70:10:10:30). The yield of carboxyparquin was 240 mg and that of parquin 102 mg.

The samples of **1** and **2** arrived from Australia as solutions in ethanol–water (1:10; v:v) containing 1% (w:v) ammonium hydroxide. After lyophilizing each three times from water to remove the bulk of the ammonium salts, the samples were stored at −10 °C. Sample purity was checked using reverse phase HPLC on Varian LC 5000 equipment monitoring at 214 nm. A gradient running from 100% water to water–acetonitrile (50:50) over 30 min was used with a Hi Chrome 4.5 × 250 mm ODS-2 column; **1** eluted after 11 min and **2** after 16 min.

Fast Atom Bombardment Mass Spectrometry.—FAB-MS spectra were recorded on Kratos MS-50 and VG 7070E instruments, fitted with standard FAB sources and Ion Tech atom guns. The samples were prepared for analysis by taking 1–2 mm^3 of methanol solution (containing 10–20 nmol of sample) and adding this directly to 2–3 mm^3 of matrix on stainless steel probe tips, ensuring thorough mixing. Xenon was used to provide the bombarding atoms which had a translation energy of 7–9 keV. Spectra were calibrated using the matrix oligomer ions of known mass. Glycerol was found to be a suitable matrix in both the positive and negative ion modes, although optimum results in positive ion mode were obtained with a mixture of glycerol and 15-crown-5-ether (95:5; v:v).[23] [$^2H_2$]Glycerol was prepared by distilling glycerol three or four times from a 1:1 (v:v) mixture of glycerol and D_2O.

All tandem mass spectra were obtained on a VG70-SEQ instrument with EBQ_1Q_2 configuration, where E is the electrostatic analyser, B is the magnet, Q_1 is an rf-only quadrupole collision cell and Q_2 is a mass filter quadrupole. Samples were ionized by fast atom bombardment (FAB) using xenon as the source of fast atoms (8.5 keV). The secondary ions produced were accelerated to 8 keV from the source region and analysed in the first mass spectrometer (EB) using a scan speed of 10 seconds/decade over the mass range 1000–60 Da at a resolution of *ca.* 2000. Parent ions were selected using EB (equivalent to MS_1) and subjected to collision activated dissociation (CAD) in Q_1. The collision gas used was argon and the gas pressure was typically *ca.* 5×10^{-6} mbar. The collision energies used were varied between 30–230 eV. Daughter ion spectra were acquired by selecting a specific ion using EB (MS_1), subjecting that ion to CAD and scanning the mass filter quadrupole Q_2 over a mass range of 1000–30 Da and 10 scans were obtained in the multi-channel analysis (MCA) mode.

NMR Spectroscopy.—NMR spectra were recorded on Bruker instruments, models WM250, WM300, AC300 and AM400. Deuteriated solvents were obtained from Aldrich Chemical Co (D_2O isotopic purity 99.96 atm % D, DMSO 99.96 atom % D). When using D_2O, samples were routinely lyophilized two or three times from D_2O and dried *in vacuo* over P_2O_5 to minimise the residual water signal. This was then removed under reduced pressure and the sample dissolved in 500 mm^3 of fresh D_2O. ^1H Homonuclear experiments were performed with 2–15 mmol dm^{-3} solutions, whereas ^{13}C–^1H correlation experiments required a 150 mmol dm^{-3} solution. It was not possible to increase the concentration much beyond this without aggregation, which caused appreciable line-broadening. ^1H and ^{13}C chemical shifts were referenced to external dioxane at δ 3.70 and 70, respectively.

1D ^1H spectra were normally recorded over 8K complex points and a spectral width of 6 ppm (δ 0–6) at all field strengths. Similarly, 1D ^{13}C spectra were recorded with 32K complex points over a spectral width of 200 ppm (δ 10–210) using composite pulse proton decoupling. DEPT spectra were acquired using standard pulse sequences.[13]

Most of the ^1H homonuclear 2D experiments (DQF-COSY, CAMELSPIN and HOHAHA) were performed in the phase sensitive mode using standard procedures.[13] These experiments employed the same spectral width as used in the one-dimensional spectra, and 32 or 64 transients of 1K quadrature pairs were acquired for each time increment (t_1). Various Lorentzian–Guassian and sinebell weighting functions were employed with zero-filling to 1K points in t_1 prior to Fourier transformation. Spectra were not symmetrized. A mixing time of 200 ms was used in the CAMELSPIN spectra, using a spin-locking field strength of 2–4 kHz. Spin-locking in HOHAHA spectra was obtained using an MLEV-17 pulse train [24] of 4–6 kHz field strength, applied for 50–100 ms. Magnitude mode COSY spectra were obtained for both **1** and **2** with the same high digital resolution as in the DQF-COSY experiments.

Heteronuclear (^1H–^{13}C) correlation experiments were performed in both conventional, ^{13}C-detected, and reverse, ^1H-detected modes. Because of the large number of ^{13}C resonances of similar chemical shift, it was preferable to work in conventional mode with the ^{13}C spectrum in v_2. The ^{13}C–^1H correlation experiments used a data size if 8K × 256 points (zero-filling once in t_1) to achieve the necessary dispersion of ^{13}C signals. Working with **1**, no weighting functions were applied prior to Fourier transformation, evolution delays were optimised for J_{CH} 150 Hz, J_{CH} 15 Hz, J_{CH} 13 Hz, J_{CH} 11.5 Hz, J_{CH} 10 Hz, J_{CH} 8.5 Hz, J_{CH} 7 Hz, J_{CH} 5 Hz, J_{CH} 3.5 Hz and J_{CH} 2.5 Hz. Each of these spectra required 24 h acquisition. Such an extensive programme was necessary to bring out all the small couplings required to complete the structure elucidation.

The ^1H-detected heteronuclear correlation experiments complemented their conventional counterparts (most correlations were seen in both modes but some were unique to one). They were performed on non-spinning samples using the pulse sequences of Bax [25] with the double difference phase cycling of Cavanagh and Keeler.[26] For one-bond correlations (HMQC) the evolution delay used was optimised for J_{CH} 150 Hz, whereas in the multiple bond experiments (HMBC) delays were optimised for J_{CH} 10 Hz, J_{CH} 7 Hz and J_{CH} 5 Hz.

Data were acquired over 1K complex points in f_2 and 512 or 1024 values of t_1 were collected. HMQC data were processed with exponential weighting functions in both dimensions, whereas unshifted sinebells produced optimum peak intensity in the HMBC experiments. All such data sets were zero-filled in t_1 prior to Fourier transformation.

Chemical Derivatization.—Selective methylation of the carboxylate groups was achieved using either diazomethane or

methyl iodide–potassium carbonate. Ethereal diazomethane was prepared by the reaction of potassium hydroxide with diazald[27] and a portion of the reagent was then added to a 5 mg sample of **1** in 200 mm^3 of methanol. This mixture was kept at 0 °C for 30 min. The solvents were then removed and the residue analysed directly by FAB-MS. For reaction with the methyl iodide–potassium carbonate, 10 mg of **1** was taken. This was suspended in 2 cm^3 of anhydrous acetone containing 250 mm^3 of methyl iodide and 25 mg of anhydrous potassium carbonate. The mixture was then heated under reflux for 6 h, cooled, and the solvents were removed under reduced pressure. The organic component was then taken up in chloroform and analysed by FAB-MS.

The hydroxy groups of **1** were acetylated by dissolving 10 mg in 500 mm^3 of pyridine and 250 mm^3 of acetic anhydride. After 24 h at room temperature, the solvents were removed under reduced pressure and the residue dried *in vacuo* over phosphorus pentoxide and potassium hydroxide. The product was taken up in chloroform and analysed by FAB-MS.

Acknowledgements

We wish to thank Schering Agrochemicals Limited and the SERC for financial support and facilities.

References

1 R. W. Purdie, D. E. Symon and L. Haegi, *Flora of Aust.*, 1982, **29**, 35.
2 H. Seifert, *Zbl. Vet. Med.*, 1960, **7**, 991.
3 T. A. Lopez, R. Spinelli and J. A. Villar, *Gac. Vet.*, 1978, **40**, 642.
4 F. Reit-Correa, A. L. Schild, M. del C. Mendez and M. H. Pinheiro, *Pesq. Vet. Brasil.*, 1986, **6**, 111.
5 J. A. Rudd and C. T. White, *Qd. Agric. J.*, 1933, **40**, 143.
6 M. W. McLennan and W. R. Kelly, *Aust. Vet. J.*, 1984, **61**, 289.
7 S. L. Everist, *Poisonous Plants of Australia*, revised edition, Angus and Robertson, Sydney, 1981.
8 T. S. Kellerman, J. A. W. Coetzer and T. W. Naude, *Plant Poisonings and Mycotoxicoses of Livestock in South Africa*, Oxford University Press, Cape Town, 1988.
9 A. R. B. Jackson, A. McInnes, I. R. Falconer and M. C. R. Runnegar, *Vet. Path.*, 1984, **21**, 102.
10 R. A. McKenzie, P. W. Dunster, J. O. Twist, C. K. Dimmock, P. B. Oelrichs, R. J. Rogers and K. R. Reichmann, *Qd. Dept. Prim. Indust. Bull.*, 1985, QB85001.
11 S. M. Thamsborg, R. J. Jorgensen and E. Brummerstedt, *Vet. Rec.*, 1987, **121**, 253.
12 K. Kudo, W. R. Kelly and P. B. Oelrichs, *Plant Toxicol., Proc. Aust. Natl. Acad. Sci., Poisonous Plants Symposium*, 1982, **34**, 179.
13 H. Kessler, M. Gehrke and C. Griesinger, *Angew. Chem., Int. Ed. Engl.*, 1988, **27**, 490.
14 D. Neuhaus, G. Wagner, M. Vasak, J. H.-P. Kagi and K. Wüthrich, *Eur. J. Biochem.*, 1985, **267**, 1151.
15 A. A. Bothner-By, R. L. Stephens, J. Lee, C. D. Warren and R. W. Jeanloz, *J. Am. Chem. Soc.*, 1984, **106**, 811.
16 A. Bax and D. G. Davis, *J. Magn. Reson.*, 1985, **63**, 207.
17 L. Braunschweiler and R. R. Ernst, *J. Magn. Reson.*, 1983, **53**, 521.
18 T. W. Goodwin and E. I. Mercer, *Introduction to Plant Biochemistry*, Pergamon, Oxford, 1983.
19 K. L. Busch, G. L. Glish and S. A. McLuckey, *Mass spectrometry/Mass spectrometry: Principles and applications of tandem mass spectrometry*, VCH Publishers, New York, 1988.
20 F. Piozzi, A. Quilico, R. Mondelli, T. Ajello, V. Sprio and A. Melera, *Tetrahedron*, 1966, Suppl. 8 II, 515.
21 F. Piozzi, A. Quilico, R. Mondelli, T. Ajello, V. Sprio and A. Melera, *Gazz. Chim. Ital.*, 1967, **97**, 935.
22 R. Santi, *Ricerca Sci.*, 1956, **26**, 2536 (*Chem. Abstr.*, 1958, **52**, 15733c).
23 S. Naylor, R. P. Mason, J. K. M. Sanders, D. H. Williams and G. Moneti, *Biochem. J.*, 1988, **249**, 573.
24 A. Bax and D. G. Davis, *J. Magn. Reson.*, 1985, **65**, 355.
25 A. Bax, A. Aszalos, Z. Dinya and K. Sudo, *J. Am. Chem. Soc.*, 1986, **108**, 8056.
26 J. Cavanagh and J. Keeler, *J. Magn. Reson.*, 1988, **77**, 356.
27 Th. J. de Boer and H. J. Backer, *Org. Synth.*, 1963, Coll. Vol. IV, 250.

Paper 1/05472D
Received 28*th October* 1991
Accepted 25*th November* 1991